TRANSVERSE MOMENTUM AND ANGULAR DISTRIBUTIONS OF HADRONS IN e^+e^- JETS FROM QCD

G. KRAMER
II. Institut für Theoretische Physik der Universität Hamburg, Hamburg, Germany

and

G. SCHIERHOLZ
Deutsches Elektronen–Synchrotron DESY, Hamburg, Germany

Received 30 October 1978

Hadron jets in e^+e^- annihilation will broaden at high energies due to gluon bremsstrahlung. With nonperturbative p_T effects dying out rapidly, the basic features of hadron jets can be calculated in perturbation theory. We examine the p_T distribution of secondarily produced hadrons. This is uniquely connected with the deviation from the $1 + \cos^2\theta$ dependence of single particle inclusive distributions. We discuss what can be learned about the gluon fragmentation given the p_T and/or angular distributions. A sum rule is derived which establishes a relationship between the average p_T^2 and α_S.

The observation of hadron jets [1,2] in e^+e^- annihilation above $\sqrt{q^2} \approx 5$ GeV gives striking evidence for the validity of the quark–parton model. In particular, the angular distribution of the jet axis with respect to the beam direction is very close to [3] $1 + \cos^2\theta$ as one would expect for the production of a pair of point-like spin-1/2 particles.

Quantum chromodynamics (QCD) is the leading candidate for the underlying field theory of the strong interactions which nicely incorporates the quark–parton model [4] and gives a natural explanation for the jet structure [5] observed in e^+e^- annihilation. With qualitative evidence abound, quantitative successes (i.e., on the quantum level) are, however, scarce. We believe that e^+e^- annihilation into hadrons is particularly suited for testing QCD in an unambiguous fashion. The main reason is that there are no spectator quarks present as in hadron–hadron and lepton–hadron scattering which spoil perturbative QCD calculations.

Recently, extensive studies of e^+e^- jet structure in QCD have evolved [5–8]. For increasing center-of-mass energies the mean transverse momentum $\langle p_T \rangle$ is expected to grow due to gluon bremsstrahlung [9] which, eventually, will give rise to a three-jet structure. This should also become visible in the one-particle inclusive cross sections. Possibly, one might even learn something about the gluon fragmentation.

To order α_S the parton model is supplemented by the diagrams shown in fig. 1 with quark and gluon momenta to be folded by their fragmentation functions. The mass singularities inherent in these diagrams, being associated with collinear quark and gluon emission, are to be absorbed into "renormalized" fragmentation functions. It has been argued in QCD perturbation theory [4] that mass singularities of inclusive cross sections factorize as required for a parton model interpretation of multi-jet processes.

In this paper we shall concentrate on the p_T distribution and angular correlations of final state hadrons. For this purpose we need not go through the procedure of infrared "renormalization". What enters here is σ_L only which (in leading order) is infrared finite [8].

The inclusive e^+e^- annihilation is described by two independent cross sections [‡1] $d\sigma_u/dx$ and $d\sigma_L/dx$

[‡1] Experimentalists sometimes use "σ_T" and "σ_L" (e.g., ref. [3]). The following relationship holds: "σ_T" = σ_u and "σ_L" = $2\sigma_L$.

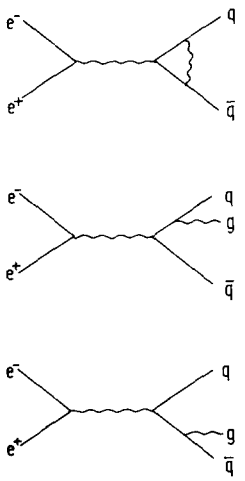

Fig. 1. Second order QCD diagrams. The vertex corrected diagram interferes with the Born graph.

(cf. [8]):

$$\frac{d^2\sigma}{d\cos\theta\, dx} = \tfrac{3}{8}(1+\cos^2\theta)\frac{d\sigma_u}{dx} + \tfrac{3}{4}(1-\cos^2\theta)\frac{d\sigma_L}{dx}. \quad (1)$$

In the free parton model (zeroth order QCD) $\sigma_L = 0$. A nonvanishing σ_L comes about because the secondary hadrons have a finite p_T with respect to the direction of the primarily produced quark–antiquark pair which smears out the $1 + \cos^2\theta$ distribution. Independent of any details of the fragmentation mechanism the angular distribution becomes for small [‡2] $\langle p_T^2\rangle/p^2$:

$$1 + \cos^2\theta + 2(\langle p_T^2\rangle/p^2) \sim 1 + \alpha(x)\cos^2\theta\ , \quad (2)$$

where

$$\langle p_T^2\rangle = \frac{\int dp_T^2 p_T^2 (d^2\sigma/dp_T^2 dx)}{\int dp_T^2 (d^2\sigma/dp_T^2 dx)}. \quad (3)$$

This provides the relationship

$$\frac{\langle p_T^2\rangle}{p^2} = \frac{1-\alpha(x)}{2\alpha(x)} = \frac{2(d\sigma_L/dx)}{(d\sigma_u/dx) - 2(d\sigma_L/dx)}. \quad (4)$$

The p_T broadening of jets has two sources: (i) Gluon bremsstrahlung (cf. fig. 1) and multi-jet structure in general and (ii) nonperturbative finite p_T effects arising from the fragmentation of quarks and gluons. It is implicitly assumed that the quark and fluon fragmentation involves a limited $\langle p_T\rangle \lesssim 400$ MeV. Since the average perturbative p_T^2 grows like [‡3] $q^2/\ln(q^2/\Lambda^2)$ nonperturbative p_T effects can asymptotically be neglected with respect to the relative p_T of quark and gluon jets.

[‡2] With a little help of geometry. See also [10]. Since, as we shall see, $\langle p_T^2\rangle/p^2 \sim \alpha_S$ this statement is correct to order α_S.

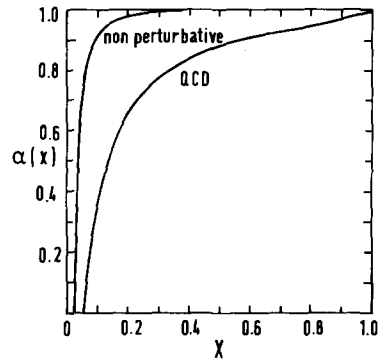

Fig. 2. Coefficient of $\cos^2\theta$ term of the single particle inclusive distribution versus x for $\sqrt{q^2} = 30$ GeV.

Hence, for large q^2 we can write

$$\frac{d\sigma_L}{dx} = \int_x^1 \frac{dx_q}{x_q}\frac{d\sigma_L}{dx_q} D_q\left(\frac{x}{x_q}\right) + \int_x^1 \frac{dx_{\bar q}}{d_{\bar q}}\frac{d\sigma_L}{dx_{\bar q}} D_{\bar q}\left(\frac{x}{x_{\bar q}}\right) + \int_x^1 \frac{dx_g}{x_g}\frac{d\sigma_L}{dx_g} D_g\left(\frac{x}{x_g}\right), \quad (5)$$

corresponding to the gluon bremsstrahlung diagrams shown in fig. 1 folded with the quark, antiquark and gluon fragmentation functions. The primordial quark, antiquark and gluon cross sections are easily computed from the results of ref. [8]. We find [‡4]

$$\frac{d\sigma_L}{dx_q} = \frac{d\sigma_L}{dx_{\bar q}} = \sigma^{(1)}\ , \quad \frac{d\sigma_L}{dx_g} = \sigma^{(1)} 4\,\frac{1-x_g}{x_g}, \quad (6)$$

where $\sigma^{(1)} = \frac{2}{3}(\alpha_S/\pi)\sigma_0$, σ_0 being the cross section for $e^+e^- \to q\bar q$ in Born approximation.

For the quark and antiquark fragmentation functions we choose the parametrization

$$xD_{q,\bar q}^{h^+ + h^-}(x) = a + b(1-x)^2\ , \quad (7)$$

[‡3] See later on.

[‡4] It is important to define the polar angle θ with respect to the quark, antiquark and gluon momenta, respectively. Here we shall assume all quark masses to be zero.

with $a = 0.05$ and $b = 1.05$ taken from Seghal's fit [11] [‡5] of $D_u^{\pi^+ + \pi^-}(x)$. We assume that the gluon fragmentation takes place via $g \to q\bar{q} \to q\bar{q}h$ which suggests $D_g^{q,\bar{q}}(x) \equiv 1$. This gives [‡6] [10]

$$xD_g^{h^+ + h^-}(x) = x\int_x^1 \frac{dz}{z} D_g^{h^+ + h^-}(z) + x\int_x^1 \frac{dz}{z} D_{\bar{q}}^{h^+ + h^-}(z)$$
$$= 2[a + b(1+x)](1-x) + 4bx \ln x \,. \quad (8)$$

With this choice of $D_q(x)$, $D_{\bar{q}}(x)$ and $D_g(x)$ we finally obtain

$$\frac{d\sigma_L^{h^+ + h^-}}{dx} = \sigma^{(1)} \frac{2}{x}\{4bx \ln^2 x - 2[2a(1+x) + b(2+3x)] \ln x$$
$$- [7a + b(13 - 3x)](1-x)\} \,. \quad (9)$$

Since our calculations are limited to first order in α_s it is sufficient to know $d\sigma_u/dx$ (eq. (4)) in zeroth order. For $\Delta\alpha(x) = 1 - \alpha(x)$ which measures the deviation of the angular distribution from the parton model result, we obtain [‡7]

$$\Delta\alpha(x) = \frac{16\alpha_s}{3\pi}\{4bx \ln^2 x - 2[2a(1+x) + b(2+3x)] \ln x$$
$$- [7a + b(13 - 3x)](1-x)\}[a + b(1-x)^2]^{-1} + O(\alpha_s^2). \quad (10)$$

The running coupling constant α_s for an arbitrary number of flavours N_f is given by

$$\alpha_s(q^2) = \frac{12\pi}{(33 - 2N_f)\ln(q^2/\Lambda^2)}, \quad (11)$$

where Λ is experimentally determined to be [‡8] $\Lambda \approx 700$ MeV. In fig. 2 we have drawn $\alpha(x)$ for $\sqrt{q^2} = 30$ GeV and five flavours which correspond to $\alpha_s = 0.22$. For comparison, also shown is the nonperturbative correction to $\alpha(x)$ as given by [‡9] (cf. eq. (4))

$$\Delta\alpha(x) = 8\frac{\langle p_T^2\rangle_{\text{nonpert.}}}{x^2 q^2}, \quad (12)$$

with $\langle p_T^2\rangle_{\text{nonpert.}} = (0.3\ \text{GeV})^2$ as measured at lower energies [3]. We find that the deviation of $\alpha(x)$ from 1 is quite substantial, while the nonperturbative effect can indeed be neglected relative to the perturbative correction. It should be said that (10) is not directly applicable for very small x ($x^2q^2 = O(m_h^2)$) since finite mass corrections to the fragmentation functions become important here.

Let us now turn to the average p_T distribution. In analogy to (10) we obtain (by use of eq. (4))

$$\langle p_T^2\rangle = \frac{2\alpha_s}{2\pi} x^2 q^2 \{4bx \ln^2 x - 2[2a(1+x) + b(2+3x)] \ln x$$
$$- [7a + b(13 - 3x)](1-x)\}[a + b(1-x)^2]^{-1} + O(\alpha_s^2) \,, \quad (13)$$

where p_T measures the transverse momentum with respect to the jet axis [‡10]. In fig. 3 we have plotted $\langle p_T^2\rangle$ for $\sqrt{q^2} = 20$ GeV and $\sqrt{q^2} = 30$ GeV. We find $\langle p_T^2\rangle$ to show (half of) a "seagull" structure [13] very similar to what has been observed, e.g., in electroproduction [14]. It peaks around $x \approx 0.7$ and for $\sqrt{q^2} = 30$ GeV increases as high as $\sqrt{\langle p_T^2\rangle} \approx 2$ GeV which is remarkably different from the parton model expectations.

The nonperturbative corrections to $\langle p_T^2\rangle$ are given by

$$\langle p_T^2\rangle = \langle p_T^2\rangle_{\text{pert.}} + \langle p_T^2\rangle_{\text{nonpert.}}$$
$$\times \frac{p^2 - \langle p_T^2\rangle_{\text{nonpert.}} - \frac{1}{2}\langle p_T^2\rangle_{\text{pert.}}}{p^2 - \langle p_T^2\rangle_{\text{nonpert.}}}. \quad (14)$$

This involves a little bit of geometry which wo do not have space to go into. We could not resist to plot the transverse momentum against the highest energy SPEAR data [3] assuming a flat $\langle p_T^2\rangle_{\text{nonpert.}} = (0.3\ \text{GeV})^2$. The result is shown in fig. 4a where $\langle p_T^2\rangle$ has been converted to $\langle p_T\rangle$ as follows. Assuming [‡11]

$$\frac{1}{\sigma}\frac{d^2\sigma}{dp_T^2 dx} = D(x)\frac{1}{p_T\sqrt{2\pi\langle p_T^2\rangle}} \exp\left(-\frac{p_T^2}{2\langle p_T^2\rangle}\right), \quad (15)$$

where $\langle p_T^2\rangle$ is allowed to be x dependent, we obtain [‡12]

[‡5] For various theoretical reasons a should actually be zero.
[‡6] If $D_{q,\bar{q}}^h(x)$ satisfies the energy sum rule $\Sigma_h \int_0^1 dx x D_{q,\bar{q}}^h(x) = 1$ so will $D_g^h(x)$.
[‡7] This is averaged over charged particles only.
[‡8] For references see [8].
[‡9] For p we take the asymptotic expression $p = x\sqrt{q^2}/2$.
[‡10] Originally, the transverse momentum was defined relative to the primordial $q\bar{q}$ direction (eq. (2)). To order α_s this definition gives the same result. Since the angle between the two axes is proportional to α_s the effect on $\langle p^2\rangle$ is of the order α_s^2.
[‡11] This has the correct behaviour as $\langle p_T^2\rangle \to 0$, i.e., $(\sqrt{2\pi\langle p_T^2\rangle})^{-1}\exp(-p_T^2/2\langle p_T^2\rangle) \to \delta(p_T)$.
[‡12] From [3] $d\sigma/dp_T^2 = C\exp(-bp_T^2)$ we obtain $\langle p_T\rangle = (\sqrt{\pi}/2)\sqrt{\langle p_T^2\rangle}$ which numerically is almost the same.

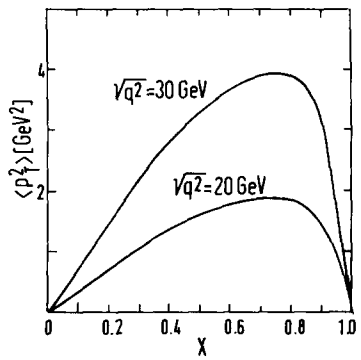

Fig. 3. Average p_T^2 versus x for $\sqrt{q^2}$ = 20 GeV and $\sqrt{q^2}$ = 30 GeV. In both cases N_f = 5.

$$\langle p_T\rangle = \sqrt{2/\pi}\,\sqrt{\langle p_T^2\rangle}\,. \tag{16}$$

There is perfect agreement with the data already at this relatively low energy.

The average transverse momentum of any particle h averaged over all x is given by

$$\langle\langle p_T\rangle\rangle_h = \frac{1}{\langle n\rangle_h \sigma}\int_0^1 dx\,\frac{d\sigma^h}{dx}\langle p_T\rangle_h\,. \tag{17}$$

Again, taking only charged particles into account we find with (16)

$$\langle\langle p_T\rangle\rangle_{h^\pm} = \frac{2}{\sqrt{3\pi}}\,\frac{\sqrt{\alpha_s q^2}}{\rho\langle n\rangle_{h^+h^-}}\int_0^1 dx\,[a+b(1-x)^2]^{1/2}$$
$$\times\{4bx\ln^2 x - 2[2a(1+x)+b(2+3x)]\ln x$$
$$-[7a+b(13-3x)](1-x)\}^{1/2}\,, \tag{18}$$

where $\rho = \frac{3}{2}\int_0^1 dx\,[a+b(1-x)^2]$. This factor corrects for the improper overall normalization [‡13] of (7) which so far cancelled out. It is straightforward how (18) is to be corrected for nonperturbative effects. Taking

$$\langle n\rangle_{h^+h^-} = 0.5\ln q^2 + 3.5\,, \tag{19}$$

from a fit to the SPEAR data [15] above charm threshold, our predictions are shown in fig. 4b which at lower energies agree well with the SPEAR [3] and PLUTO [2] data.

‡13 Note that $\int_0^1 dx\,[a+b(1-x)^2] = 0.4$ for $a = 0.05$ and $b = 1.05$ which, for our use, should be 2/3.

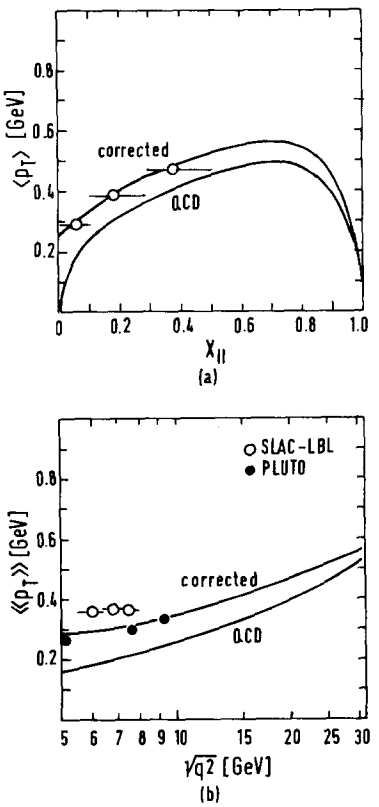

Fig. 4. (a) Average p_T versus x compared to the SPEAR data [3] for $7.0 < \sqrt{q^2} < 7.8$ GeV. (b) Average p_T averaged over all x versus $\sqrt{q^2}$ compared to the SPEAR [3] and PLUTO [2] data. N_f = 4 below 10 GeV.

The weakest link in our set of predictions so far is the gluon fragmentation function $D_g(x)$. One could turn the tables now and try to determine $D_g(x)$ from measurements of $\alpha(x)$ or $\langle p_T^2\rangle$. Eventually, thus will give some further evidence for QCD. In particular, one might test if gluons are flavour blind as one expects them. This might also be a place where to search for glue-balls.

From eqs. (4)–(6) and

$$\frac{d}{dx}x^2\frac{d}{dx}\int_x^1\frac{dz}{z}\frac{(1-z)}{z}D_g\left(\frac{x}{z}\right) = D_g(x)\,, \tag{20}$$

we obtain

$$D_g^h(x) = \frac{d}{dx}\left\{\frac{3\pi}{64\alpha_s}x^2\frac{d}{dx}[(D_g^h(x)+D_{\bar{q}}^h(x))\Delta\alpha(x)]\right.$$

$$\left.+\frac{x}{4}(D_g^h(x)+D_{\bar{q}}^h(x))\right\} = \frac{d}{dx}\left\{\frac{3\pi}{32\alpha_s}x^2\frac{d}{dx}\left[\frac{1}{\sigma}\frac{d\sigma^h}{dx}\Delta\alpha(x)\right]\right.$$

$$\left.+\frac{x}{2}\frac{1}{\sigma}\frac{d\sigma^4}{dx}\right\} + O(\alpha_s)\,, \qquad (21)$$

or, alternatively, $\Delta\alpha(x)$ replaced by $8\langle p_T^2\rangle/x^2q^2$ (cf. eq. (4)). In trems of moments, which are more useful for experimental studies, this reads

$$[D_g^h]^{(n)} \underset{n>0}{=} \frac{3\pi n(n+1)}{4\alpha_s q^2}\left[\frac{1}{\sigma}\frac{d\sigma^h}{dx}\langle p_T^2\rangle\right]^{(n-2)}$$

$$-\frac{n}{2}\left[\frac{1}{\sigma}\frac{d\sigma^h}{dx}\right]^{(n)} + O(\alpha_s)\,, \qquad (22)$$

where

$$[f(x)]^{(n)} = \int_0^1 dx x^n f(x)\,. \qquad (23)$$

In practice it should be sufficient to evaluate a few moments only for reconstructing $D_g(x)$ to a certain accuracy. For testing global features of QCD (such as the flavour blindness of gluons which would involve verifying, e.g., $D_g^{K^\pm}(x) = D_g^{K^0}(x) = D_g^{\eta}(x)$ or $D_g^p(x) = D_g^n(x)$) it would even be enough to consider one of the lower moments.

Let us conclude our investigation with what we believe to be the most straightforward (experimentally) and unambiguous test of QCD in this context. As a matter of energy conservation the fragmentation functions are normalized according to

$$\sum_h \int_0^1 dx x D_\lambda^h(x) = 1, \quad \lambda = q, \bar{q}, g\,. \qquad (24)$$

Hence, putting $n = 1$, the fragmentation functions drop out from (22) and we obtain the *sum rules*

$$\sum_h \int_0^1 \frac{dx}{x}\frac{1}{\sigma}\frac{d\sigma^h}{dx}\langle p_T^2\rangle = \frac{\alpha_s}{\pi}q^2 + O(\alpha_s^2) \qquad (25)$$

and

$$\sum_h \int_0^1 dx x \frac{1}{\sigma}\frac{d\sigma^h}{dx}\Delta\alpha(x) = \frac{8\alpha_s}{\pi} + O(\alpha_s^2)\,. \qquad (26)$$

If charged particles are detected only the right-hand side of (25) and (26) has to be multiplied by their appropriate ratio. Eqs. (25) and (26) can also be more directly derived from (4) and

$$\sum_h \int_0^1 dx x \frac{d\sigma_L^h}{dx} = \frac{2\alpha_s}{\pi}\sigma + O(\alpha_s^2)\,, \qquad (27)$$

which follows from (5).

The sum rule (26) is relatively easy to test as one does not have to go through a complete jet analysis. High statistics is desirable though in order to establish the $\ln q^2$ dependence of α_s. This should be feasible in the range 20 GeV $\lesssim \sqrt{q^2} \lesssim t\bar{t}$-threshold where finite mass corrections are expected to be negligible.

It is certainly no accident that the same kind of jet structure as predicted for e^+e^--annihilation is found in electroproduction [14] and at the ISR [16] ("sea-gull" effect). This needs further investigation.

References

[1] G.G. Hanson et al., Phys. Rev. Lett. 35 (1975) 1609.
[2] Ch. Berger et al., Phys. Lett. 78B (1978) 176.
[3] G.G. Hanson, SLAC preprints, SLAC-PUB 1814 (1976); SLAC-PUB 2118 (1978); and in: Proc. of the 13th Rencontre de Moriond on High Energy Leptonic Interactions and High Energy Hadronic Interactions, Les Arcs, March 12–24, 1978, to be published.
[4] E.g., R.K. Ellis et al., MIT preprint CTP 718 (1978).
[5] G. Sterman and S. Weinberg, Phys. Rev. Lett. 39 (1977) 1436.
[6] A. De Rujula et al., Nucl. Phys. B138 (1978) 387.
[7] S.-Y. Pi, R.L. Jaffe and F.E. Low, Phys. Rev. Lett. 41 (1978) 142.
[8] G. Kramer, G. Schierholz and J. Willrodt, DESY preprint DESY 88/36 (1978), to be published in Phys. Lett. B.
[9] H.D. Politzer, Phys. Lett. 70B (1977) 430.
[10] R.P. Feynman, Photon–hadron interaction (Benjamin, Reading, 1972);
M. Gronau, T.F. Walsh, Y. Zarmi and W.S. Lam, Nucl. Phys. B104 (1976) 307;
U. Sukhatme and J. Tran Thanh Van, Orsay preprint LPTPE 78/4 (1978).
[11] L.M. Seghal, in: Proc. of the 1977 International Symposium on Lepton and Photon Interactions at High Energies, Hamburg (ed. F. Gutbrod) p. 837.
[12] Cf. K. Koller and T.F. Walsh, Phys. Lett. 72B (1977) 227; Erratum 73B (1978) 504.
[13] L.N. Hand, in: Proc. of the 1977 International Symposium on Lepton and Photon Interactions at High Energies, Hamburg (ed. F. Gutbrod) p. 417.
[14] C.K. Chen et al., Nucl. Phys. B133 (1978) 13;
C. del Papa et al., Phys. Rev. D15 (1977) 2425.
[15] V. Lüth, in: Proc. of the Summer Instituet on Particle Physics, SLAC, July 11–22, 1977 (ed. M. Zipf) p. 219.
[16] M. Della Negra et al., Nucl. Phys. B127 (1977) 1.